Dependency of the Delocalized Charge Density and of the Structural Parameters on the Pseudorotational Parameter φ in 1,1-Dicyanocyclopentane

Volker Typke*,† and Marwan Dakkouri*,‡

Communication and Information Center, University of Ulm, D-89069 Ulm, Germany, and Department of Electrochemistry, University of Ulm, D-89069 Ulm, Germany

Received: April 22, 2005; In Final Form: July 18, 2005

Encouraged by the results we recently obtained from the exploration of the dependency of the structural parameters of 1,1-dichlorocyclopentane (*J. Chem. Phys. A* **2004**, *108*, 4658) on the pseudorotational parameter φ, we decided to reinvestigate the structure and the potential function governing the conformational equilibrium of 1,1-dicyanocyclopentane (DCCP) in the light of these novel results. The improved potential function we developed describes more adequately the dependency of the geometrical parameters on the pseudorotational phase angle φ. In the present work, we also incorporated additional terms into the equations we developed earlier (*J. Chem. Phys. A* **2004**, *108*, 4658; *J. Mol. Struct.* **2002**, *612*, 181) for describing the dependency of the distribution of the delocalized net charges throughout the ring on φ to account for the observed systematic deviations between the computed atomic distances and those provided by these equations. Although the overall fit of the electron diffraction was not significantly different from that which we presented previously, however, applying these extended equations has led to a better fit by refining a smaller number of parameters.

1. Introduction

The large amplitude motion in cyclopentane, which is referred to as pseudorotation was first suggested and treated quantitatively by Pitzer[3] and Kilpatrick, Pitzer, and Spitzer.[4] A more detailed treatment of the pseudorotational motion was later undertaken by Harris et al.[5] The numerous investigations of this particular large amplitude motion by means of spectroscopic and diffraction methods have been repeatedly reviewed.[6−9]

Very recently we published a paper on the molecular structure of 1,1-dicyanocyclopentane (DCCP).[2] In this work, we studied the dependency of various structural parameters on the pseudorotational motion in this molecule. All quantum mechanical methods we applied in this investigation have revealed that DCCP exists in the C_s symmetric form as well as in the C_2 form. There it has been shown that the proportion of the C_2 conformer is determined by the values of the potential parameters V_2 and V_4 associated with the potential for the hindered pseudorotational motion in this five-membered ring molecule. Therefore, we adjusted the potential parameter V_4 from the experimental electron diffraction data while keeping V_2 fixed to the ab initio value. Furthermore, to account for the unexpectedly considerable dependency of the ring parameters on the pseudorotational motion, we introduced a density function $d(\alpha,\varphi)$ which describes the dependency of the distribution of the delocalized net charges throughout the ring on the pseudorotational parameter, the phase angle φ.

In continuation of this work, we studied the molecular structure of 1,1-dichlorocyclopentane (DClCP) by means of gas-phase electron diffraction and ab initio calculations.[1] We found that for DClCP the C_2 symmetry is not a minimum in the energy hypersurface of the pseudorotational motion, but a saddle point. This was clearly seen by calculating the energies at various values of the pseudorotational puckering amplitude q with φ ranging from 0 to 360°. Consequently, when the vibrational spectrum for the C_2 symmetric form was calculated, an "imaginary" vibration was found.

On the basis of these results, we decided to reinvestigate DCCP and to calculate the energy hypersurface for the pseudorotational motion. It turned out that also in DCCP the energy hypersurface exhibits a saddle point at the C_2 symmetry, and consequently, a complete reanalysis of the molecular structure of DCCP was required.

2. Experimental Data

The experimental data we used in the present study are those which we already described in the previous paper.[2] The usual data reduction and refinement procedures of the electron diffraction data were used,[10,11] and the atomic scattering amplitudes and phases of Haase[12] were applied.

3. Dependency of Geometry on Pseudorotation

In the previous paper,[1] we described in detail the steps for the evaluation of the hindering potential for the pseudorotational motion and the dependency of the molecular geometry—including the puckering amplitude q—on the phase angle φ. Therefore, in the present paper, we give only a short outline.

The corresponding ab initio calculations were performed using the package MOLPRO.[13] This package provides a convenient way to include functional dependencies with the input data, and thus the pseudorotation can be easily treated. The methods HF/cc-pVDZ and MP2/cc-pVDZ have been applied. In Table 1 are collected the calculated energies using the HF/cc-pVDZ at various values of the parameters q and φ, and Figure 1 shows a graphical presentation of these data. The dashed line indicating the bottom of the energy valley corresponds to the minimum energy at a given value of the phase angle φ, and therefore the

† Communication and Information Center, University of Ulm.
‡ Department of Electrochemistry, University of Ulm.

10.1021/jp0520897 CCC: $30.25
Published on Web 09/07/2005

TABLE 1: Calculated Energies (cal/mol) for 1,1-dicyanocyclopentane at Various Values of the Pseudorotational Puckering Amplitude q and Pseudorotational Phase φ (Basis Set HF/cc-pVDZ)

φ	0.37	0.38	0.39	0.40	0.41	0.418 24	0.42	0.43	0.44	0.45	0.46
110	919.1	824.6	750.0	696.8	666.5	659.8	660.6	680.5	727.7	803.8	910.1
130	718.2	630.9	565.3	523.1	505.7	511.1	514.6	551.6	617.8	715.0	844.7
150	478.4	394.9	334.5	298.5	288.6	301.0	306.2	353.0	430.3	539.6	682.1
170	267.5	176.3	107.8	63.2	44.2	48.9	52.3	88.9	155.5	253.1	383.4
190	267.6	176.3	107.9	63.3	44.4	49.0	52.4	88.9	155.1	252.8	383.1
210	478.3	394.8	334.4	298.4	288.5	300.9	306.1	352.9	430.2	539.5	682.1
230	717.9	630.8	565.2	523.0	505.7	511.1	514.6	551.5	617.7	715.0	844.6
250	919.3	824.7	750.1	696.9	666.6	660.0	660.7	680.6	727.8	803.8	910.0
270	1010.3	914.1	837.2	781.0	747.1	736.8	736.8	751.7	793.0	862.5	961.5
275	1004.5	908.3	831.5	775.6	741.9	731.9	731.8	746.9	788.6	858.4	957.8
280	986.0	890.1	813.7	758.3	725.2	715.8	715.9	731.9	774.6	845.6	946.2
300	824.9	733.3	662.5	614.0	586.2	587.8	589.7	617.1	672.7	757.9	874.7
320	602.3	518.8	457.6	420.7	409.4	420.7	425.3	470.0	544.9	651.5	791.1
340	358.0	271.1	207.3	167.7	154.0	163.5	167.9	210.7	283.8	388.4	526.2
355	242.2	149.5	79.4	33.2	12.4	12.4	18.5	52.9	117.1	212.4	340.0
360	233.3	140.2	69.5	22.7	1.3	5.0	6.7	40.2	103.5	197.7	324.5

energy values represent the potential function of the pseudorotation. At the same time this line corresponds to the optimal value q_{min} of the puckering amplitude at a given phase angle φ. A Fourier analysis of $V(\varphi) = E_{min}(\varphi)$ and $q_{min}(\varphi)$ yields the coefficients collected in Table 2 where $V(\varphi)$ and $q(\varphi)$ are assumed to be of the form

$$V(\varphi) = {}^1/_2V_2(1 - \cos 2\varphi) + {}^1/_2V_4(1 - \cos 4\varphi) + {}^1/_2V_6(1 - \cos 6\varphi) \quad (1)$$

$$q(\varphi) = q_0 + q_2 \cos 2\varphi + q_4 \cos 4\varphi + q_6 \cos 6\varphi \quad (2)$$

In Figure 2, we show the potential function $V(\varphi)$; this figure also includes the potential function resulting from the MP2/cc-pVDZ calculations.

It is obvious that optimizing the molecular geometry at $q_{min}(\varphi)$ provides all geometrical parameters for the complete cycle of pseudorotation. This offers the possibility to analyze the variation of the molecular geometry due to the pseudorotation. For brevity we restrict this analysis to the results obtained with the HF/cc-pVDZ method.

As is obvious from Table 2 in the previous paper,[2] the ring C−C bond lengths depend markedly on the molecular symmetry, i.e., on the phase angle φ. To rationalize this finding, we presented very recently[1,2] a model which assumes that these changes are induced by changes in the density distribution of the delocalized net charges, which represents the overall

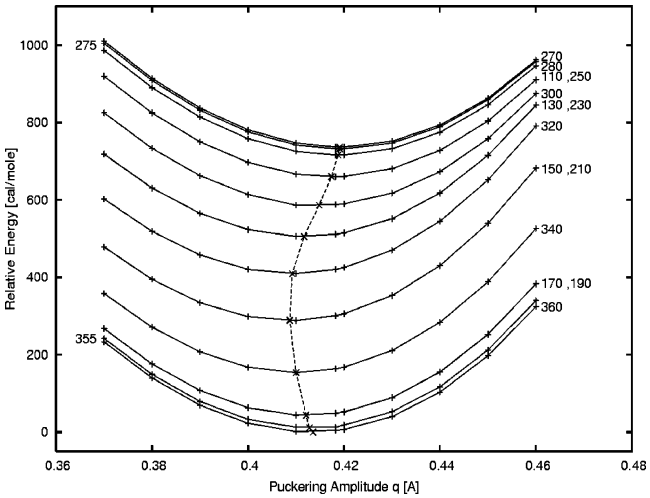

Figure 1. Dependency of the energy on the puckering amplitude q and the puckering phase angle φ.

TABLE 2: Minimal Value of Pseudorotational Puckering Amplitude q and Energy (cal/mol) at Various Values of Pseudorotational Phase Angle φ, and Fourier Coefficients of the Puckering Amplitude q (Å, Eq 2) and of the Potential Curve $V(\varphi)$ (cal/mol, Eq 1)[a]

	HF/cc-pVDZ		MP2/cc-pVDZ	
φ	q_{min}	E_{min}	q_{min}	E_{min}
110	0.4174	659.7		
130	0.4117	505.3		
150	0.4087	289.9		
170	0.4121	43.6		
190	0.4121	43.8		
210	0.4087	288.2		
230	0.4117	505.3		
250	0.4174	659.8		
270	0.4191	736.7	0.4470	1144.1
275	0.4191	731.7	0.4470	1133.5
280	0.4188	715.7	0.4470	1101.1
300	0.4148	586.2	0.4445	845.5
320	0.4092	409.3	0.4390	561.0
340	0.4100	154	0.4407	217.3
355	0.4128	11.3	0.4451	16.1
360	0.4135	0.0	0.4455	0.0
Fourier Coefficients				
order	$q(\varphi)$	$V(\varphi)$	$q(\varphi)$	$V(\varphi)$
0	0.4132	0.0	0.4408	0.0
2	−0.0081	690.1	−0.0050	1061.3
4	0.0059	91.6	0.0062	64.1
6	0.0022	47.4	0.0035	84.1

[a] Only a limited number of calculations were performed using the MP2/cc-pVDZ method.

distribution of charges throughout the ring. Thus, we write for the ring bond distance C_i-C_j

$$r_{ij}(\varphi) = r_{CC} + \int_{\alpha_i}^{\alpha_j} d(\alpha,\varphi)\, d\alpha \quad (3)$$

where the density distribution is given by

$$d(\alpha,\varphi) = d_1 \cos\alpha + d_2 \cos 2\alpha + d_{2c} \cos 2\varphi + d_{c2c} \cos\alpha \cos 2\varphi + d_{s2s} \sin\alpha \sin 2\varphi + d_{c4c} \cos\alpha \cos 4\varphi + d_{s4s} \sin\alpha \sin 4\varphi + d_{2c2c} \cos 2\alpha \cos 2\varphi + d_{2s2s} \sin 2\alpha \sin 2\varphi + d_{2c4c} \cos 2\alpha \cos 4\varphi + d_{2s4s} \sin 2\alpha \sin 4\varphi \quad (4)$$

In eqs 3 and 4, α designates the angle between a line from the center of the ring to atom C_1 and a line to every other position on the ring, both projected to the mean plane as defined by

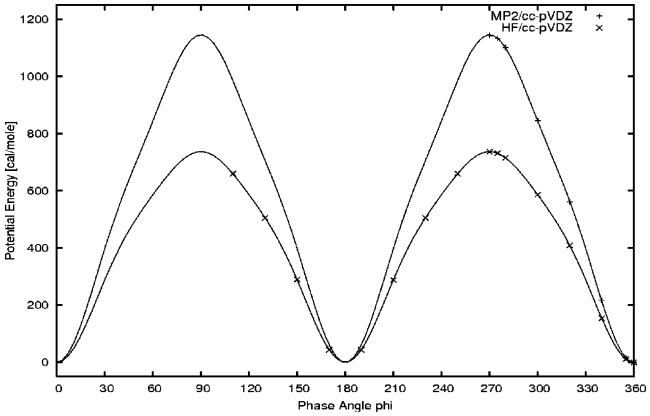

Figure 2. Potential function for the pseudorotation in 1,1-dicyanocyclopentane (angles in degree) calculated with the HF/cc-pVDZ method and the MP2/cc-pVDZ method.

TABLE 3: Fitted Constants from Eq 4 for 1,1-Dicyanocyclopentane and 1,1-Dichlorocyclopentane (Data from Ref 1)

parameter	DCCP	DClCP
r_{CC}	1.5453	1.5369
d_1	0.0120	−0.0027
d_2	0.0067	0.0008
d_{2c}	−0.0003	−0.0003
d_{c2c}	−0.0106	−0.0107
d_{c4c}	0.0001	0.0004
d_{s2s}	−0.0098	−0.0097
d_{s4s}	0.0003	0.0009
d_{2c2c}	−0.0006	−0.0002
d_{2c4c}	0.0021	0.0020
d_{2s2s}	−0.0007	−0.0009
d_{2s4s}	0.0023	0.0025

Cremer and Pople.[14] For the cyclopentane derivatives studied thus far it is a sufficiently good approximation to assume a regular pentagon in the mean plane of the five-membered ring. Particularly in the case of DCCP the uppermost deviation of the angles α from their respective value in a regular pentagon is 0.75°. If we adjust the parameters r_{CC}, d_1, d_2, etc. such that all ab initio ring distances are optimally reproduced by applying a least squares procedure we obtain the results shown in column 1 of Table 3.

Compared to the relatively simple formula given previously,[2] eq 4 includes more terms in order to cover the values of all ring C−C bond distances during one cycle of pseudorotation.

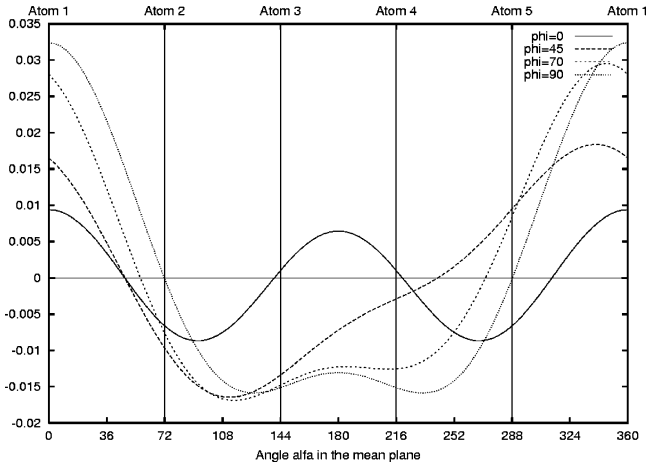

Figure 3. Density of the delocalized net charge distribution for $\varphi = 0°$, $\varphi = 45°$, $\varphi = 70°$, and $\varphi = 90°$.

TABLE 4: Fourier Coefficients for the Ring C−C Bond Distances (Eq 5) and the C−C−C Bond Angles (Eq 6)

parameter	r_{12}, r_{15}	r_{23}, r_{45}	r_{34}
δr_{ij}	0.0134	−0.0095	−0.0077
$c_{2,ij}$	−0.0107	0.0040	0.0116
$c_{4,ij}$	0.0007	−0.0016	0.0018
$s_{2,ij}$	−0.0074	−0.0105	0.0
$s_{4,ij}$	0.0023	−0.0009	0.0
parameter	α_{123}, α_{451}	α_{234}, α_{345}	α_{512}
$\alpha_{0,ijk}$	104.40	104.85	103.79
$c_{2,ijk}$	−0.33	1.42	−1.58
$c_{4,ijk}$	0.07	−0.10	−0.19
$s_{2,ijk}$	−1.48	−1.13	0.0
$s_{4,ijk}$	−0.09	0.16	0.0

Furthermore, compared to the function given in ref 1, an additional term with coefficient d_{2c} has been included to account for systematic deviations between the bond distances obtained from the quantum mechanical procedures and by applying a formula without this term. In Figure 3, we show the function $d(a, \varphi)$ (we regret that in ref 2, the wrong figure has been included for visualization of the density function) for the phase angles $\varphi = 0$, 45, 70, and 90°. To interpret this figure we note that the integral of the curve for $\varphi = 0°$ between atoms 3 and 4 is clearly positive, while the integral between atoms 2 and 3 and between atoms 4 and 5 is clearly negative: this means that between atoms 3 and 4 the electronic charge has been decreased, leading to a bond distance longer than the average distance r_{CC}, while the opposite is true for the bond lengths r_{23} and r_{45}. Similarly the bond lengths r_{23}, r_{34}, and r_{45} for $\varphi = 90°$ are shorter than r_{CC}, while the bond bond lengths r_{12} and r_{15} are considerably longer.

Combining the values of the integrals and the constants from eq 4 we find that the ring C−C bond distances vary as

$$r_{ij}(\varphi) = r_{CC} + \delta r_{ij} + c_{2,ij}\cos 2\varphi + c_{4,ij}\cos 4\varphi \pm s_{2,ij}\sin 2\varphi \pm s_{4,ij}\sin 4\varphi \quad (5)$$

It is straightforward to verify that the parameters of eqs 4 and 5 are related by

$$\delta r_{ij} = d_1(\sin\alpha_j - \sin\alpha_i) + {}^1/_2 d_2(\sin 2\alpha_j - \sin 2\alpha_i)$$

$$c_{2,ij} = d_{c2c}(\sin\alpha_j - \sin\alpha_i) + {}^1/_2 d_{2c2c}(\sin 2\alpha_j - \sin 2\alpha_i) + d_{2c}(\alpha_j - \alpha_i)$$

$$c_{4,ij} = d_{c4c}(\sin\alpha_j - \sin\alpha_i) + {}^1/_2 d_{2c4c}(\sin 2\alpha_j - \sin 2\alpha_i)$$

$$s_{2,ij} = -d_{s2s}(\cos\alpha_j - \cos\alpha_i) - {}^1/_2 d_{2s2s}(\cos 2\alpha_j - \cos 2\alpha_i)$$

$$s_{4,ij} = -d_{s4s}(\cos\alpha_j - \cos\alpha_i) - {}^1/_2 d_{2s4s}(\cos 2\alpha_j - \cos 2\alpha_i)$$

The coefficients of eq 5 have been included in Table 4.

The deformation of the ring is further characterized by the changes in the C−C−C bond angles. A Fourier analysis of the calculated C−C−C bond angles according to the equation

$$\alpha_{ijk}(\varphi) = \alpha_{0,ijk} + c_{2,ijk}\cos 2\varphi + c_{4,ijk}\cos 4\varphi \pm s_{2,ijk}\sin 2\varphi \pm s_{4,ijk}\sin 4\varphi \quad (6)$$

yields the coefficients included in Table 4.

With regard to the variation of geometrical parameters involving ligands attached to the ring C atoms we find that Fourier coefficients up to fourth order are adequate. For the

C−C≡ bonds we find that these bond distances are well reproduced by the equation

$$r_{CC\equiv}(\varphi) = R_0 \pm R_1 \cos\varphi + R_2 \cos 2\varphi \pm R_3 \cos 3\varphi + R_4 \cos 4\varphi \quad (7)$$

This formula is valid for both the axial and the equatorial positions of the C−C≡ bond: the upper sign corresponds to the C_1-C_6 bond, the lower sign to the C_1-C_8 bond (for numbering of atoms cf. Figure 4). In Table 5 the coefficients R_0 through R_4 are listed.

Concerning the C−H bond lengths a Fourier analysis of the calculated C−H bond lengths shows that the dependency on φ is too small to be extracted from electron diffraction data. The variation of these distances has led exclusively to an increase of the observed vibrational amplitudes l(C−H). The same is true for the variations of the H−C−H bond angles. Therefore, in the analysis of the ED data, both parameters were considered in zeroth order only. Further, we find that the C≡N bond lengths and the C−C≡N bond angles are almost independent of the phase angle φ, and these parameters were also considered exclusively in zeroth order.

However, with respect to intramolecular angles, it is important to include the variations of the rocking (ρ), wagging (ω), and twisting (τ), angles as defined by Skancke et al.[15] in addition to the ring C−C−C angles and the angle $\beta = C_6-C_1-C_8$. For the angles in the $C(CN)_2$ group we used the following functions:

$$\begin{aligned} \beta(\varphi) &= \beta_0 + \beta_2 \cos 2\varphi + \beta_4 \cos 4\varphi \\ \rho(\varphi) &= \rho_1 \cos\varphi + \rho_3 \cos 3\varphi \\ \omega(\varphi) &= \omega_2 \sin 2\varphi + \omega_4 \sin 4\varphi \\ \tau(\varphi) &= \tau_1 \sin\varphi + \tau_3 \sin 3\varphi \end{aligned} \quad (8)$$

Table 5 also includes the resulting coefficients β_0 through τ_3. Similarly for the deformations of the CH_2 groups we used the functions

$$\rho_{C2,5}(\varphi) = \rho_{2,c1}\cos\varphi + \rho_{2,c3}\cos 3\varphi \pm \rho_{2,s1}\sin\varphi \pm \rho_{2,s3}\sin 3\varphi$$

$$\rho_{C3,4}(\varphi) = \rho_{3,c1}\cos\varphi + \rho_{3,c3}\cos 3\varphi \pm \rho_{3,s1}\sin\varphi \pm \rho_{3,s3}\sin 3\varphi$$

$$\omega_{C2,5}(\varphi) = \pm\omega_{2,0} \pm \omega_{2,c2}\cos 2\varphi \pm \omega_{2,c4}\cos 4\varphi + \omega_{2,s2}\sin 2\varphi + \omega_{2,s4}\sin 4\varphi \quad (9)$$

$$\omega_{C3,4}(\varphi) = \pm\omega_{3,0} \pm \omega_{3,c2}\cos 2\varphi \pm \omega_{3,c4}\cos 4\varphi + \omega_{3,s2}\sin 2\varphi + \omega_{3,s4}\sin 4\varphi$$

$$\tau_{C2,5}(\varphi) = \pm\tau_{2,c1}\cos\varphi \pm \tau_{2,c3}\cos 3\varphi + \tau_{2,s1}\sin\varphi + \tau_{2,s3}\sin 3\varphi$$

$$\tau_{C3,4}(\varphi) = \pm\tau_{3,c1}\cos\varphi \pm \tau_{3,c3}\cos 3\varphi + \tau_{3,s1}\sin\varphi + \tau_{3,s3}\sin 3\varphi$$

The coefficients in these formulas are displayed in Table 6.

4. Reanalysis of Electron Diffraction Data

We restrict the reanalysis to the large amplitude treatment presented in the previous paper[2] and similarly was restricted for 1,1-dichlorocyclopentane.[1] However, since the dependency of all geometrical parameters on φ is now available, we included additional information from the treatment in the previous chapter. Thus, the reanalysis is based on the following model:

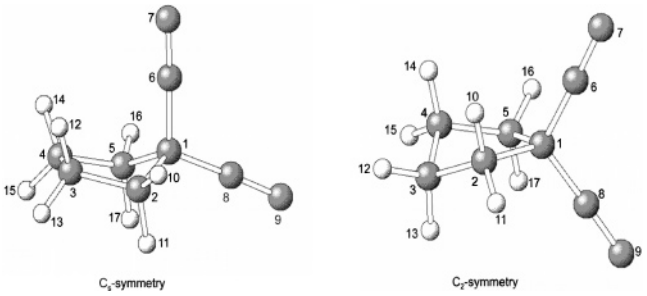

Figure 4. Atomic numbering of 1,1-dicyanocyclopentane (DCCP).

TABLE 5: Deformation of the Cyano Group with the Phase Angle φ: the Fourier Coefficients of the Geometrical Parameters (Eqs 7 and 8)

order	R	β	ρ	ω	τ
0	1.4792	108.67	0.00	0.00	0.00
1	0.0031	0.00	−5.74	0.00	−0.04
2	0.0003	0.26	0.00	0.59	0.00
3	−0.0004	0.00	1.30	0.00	0.76
4	−0.0002	0.09	0.00	−0.45	0.00

TABLE 6: Deformation of the CH_2 Groups with the Phase Angle φ: Fourier Coefficients of the Geometrical Parameters (Eq 9)

order	$\rho_{C2,5}$	$\omega_{C2,5}$	$\tau_{C2,5}$	$\rho_{C3,4}$	$\omega_{C3,4}$	$\tau_{C3,4}$
0	0.00	−5.03	0.00	0.00	−1.38	0.00
c1	8.09	0.00	1.05	−1.19	0.00	0.78
c2	0.00	−0.49	0.00	0.00	−0.21	0.00
c3	0.15	0.00	1.15	−1.07	0.00	0.95
c4	0.00	0.12	0.00	0.00	−0.20	0.00
s1	−5.41	0.00	−0.26	−5.70	0.00	0.93
s2	0.00	0.02	0.00	0.00	−0.31	0.00
s3	1.56	0.00	0.57	−0.66	0.00	−1.13
s4	0.00	0.16	0.00	0.00	−0.04	0.00

The ring geometry at a chosen value of φ is calculated from the ring C−C bond distances, the bond angle α_{512}, the puckering amplitude q, and the phase angle φ. The bond angle α_{123} was maintained such that C_s symmetry at $\varphi = 0°$ is guaranteed. Also, for the $C(CN)_2$ and all CH_2 groups the rocking, wagging, and twisting angles were utilized. For most of the parameters, the Fourier coefficients collected in Tables 2−6 were applied in the calculations. However, as stated in the previous section, the bond distances C−H and C≡N as well as the bond angles H−C−H and C−C≡N are almost independent of the phase angle φ, and they were considered only in zeroth order.

The vibrational amplitudes l_{ij} and the corrections $\delta_{ij} = (r_{a,ij} - r_{\omega,ij})$ have been calculated in the range $-90° \le \varphi \le +90°$ using the ab initio force field of the most stable conformer of C_s symmetry. However, in the analysis of the ED data differences l_{ij} ($\varphi \neq 0°$) − l_{ij} ($\varphi = 0°$) of the calculated vibrational amplitudes were used in the same way as reported in the previous papers.[1,2]

To account for large amplitude motions in the analysis of gas-phase electron diffraction data the assumption is made that the reduced total molecular intensity $s*M(s)$ can be written as

$$s*M(s) = \int_0^{2\pi} w(\varphi)\, s*M(s,R(\varphi))\, d\varphi \Big/ \int_0^{2\pi} w(\varphi)\, d\varphi \quad (10)$$

where $R(\varphi)$ designates the geometry of the molecule at the phase

TABLE 7: Final Fitted Model Parameters (r_a, r_α) and Errors for 1,1-Dicyanocyclopentane Using the Pseudorotational Model[g]

	r_a fit				r_α fit			
	value	σ_1 [a]	σ_2 [b]	σ_{total} [c]	value	σ_1 [a]	σ_2 [b]	σ_{total} [c]
			Geometrical Parameters (Distances in Å, Angles in deg)					
r_{CC}	1.550	0.001	0.001	0.003	1.546	0.001	0.001	0.003
q[d]	0.437	0.007	0.008	0.021	0.448	0.005	0.010	0.021
C−C≡	1.470	0.002	0.002	0.006	1.472	0.002	0.002	0.005
C≡N	1.164	0.001	0.000	0.002	1.149	0.001	0.000	0.002
C−H[e]	1.081	0.002	0.000	0.005	1.065	0.001	0.000	0.003
α_{512}	104.3	0.5	0.4	1.4	103.4	0.4	0.4	1.2
NC−C−CN	108.8	0.5	1.0	2.1	109.6	0.4	1.1	2.2
H−C−H	110.0	1.0	0.5	2.6	109.6	0.8	0.4	2.0
C−C≡N	173.1	0.8	0.7	2.3	174.7	0.6	1.0	2.3
			Fitted Vibrational Amplitudes (Å)					
l(C−C_{ring})	0.056	0.001	0.001	0.003	0.057	0.001	0.001	0.003
l(C−C≡)	0.049	0.003	0.001	0.007	0.048	0.002	0.001	0.005
l(C−H)	0.082	0.003	0.000	0.006	0.079	0.002	0.000	0.005
l(C≡N)	0.033	0.001	0.000	0.002	0.031	0.001	0.000	0.001
l(C_2···C_8)	0.077	0.005	0.005	0.014	0.073	0.003	0.005	0.012
l(C_1···N_7)	0.058	0.003	0.002	0.007	0.054	0.002	0.002	0.006
l(C_2···N_9)	0.113	0.003	0.006	0.013	0.110	0.002	0.006	0.011
l(C_1···H_{10})	0.109	0.002	0.001	0.006	0.108	0.002	0.001	0.004
R_{long} [f]	2.48				1.85			
R_{short} [f]	4.94				3.87			

[a] σ_1 is the single standard error of the fit. [b] σ_2 is the propagated error (see refs 16−18). [c] $\sigma_{total} = (6\sigma_1^2 + 3\sigma_2^2)^{1/2}$. [d] Puckering amplitude. [e] Average value $(r_{2,0} + r_{3,0})/2$. [f] $R = [\sum w_i \Delta_i^2/\sum(w_i s^2 M_i^2(\text{obs}))]^{1/2}$, where $\Delta_i = sM_i(\text{obs}) - sM_i(\text{calc})$. [g] Note that for several parameters only the zeroth order contributions according to eqs 2, and 6−8 have been fitted.

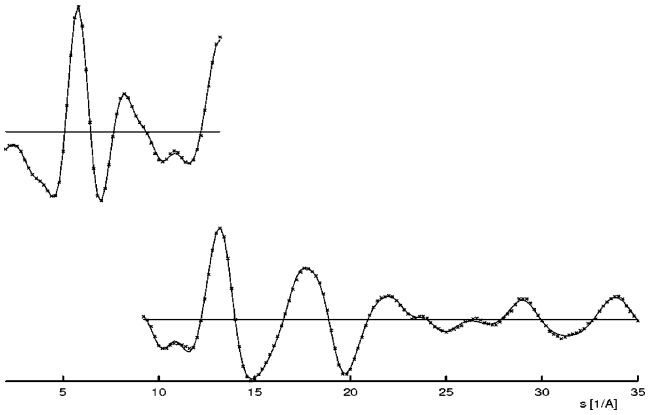

Figure 5. Experimental (×) and theoretical (−) reduced molecular intensity $s*M(s)$ for DCCP.

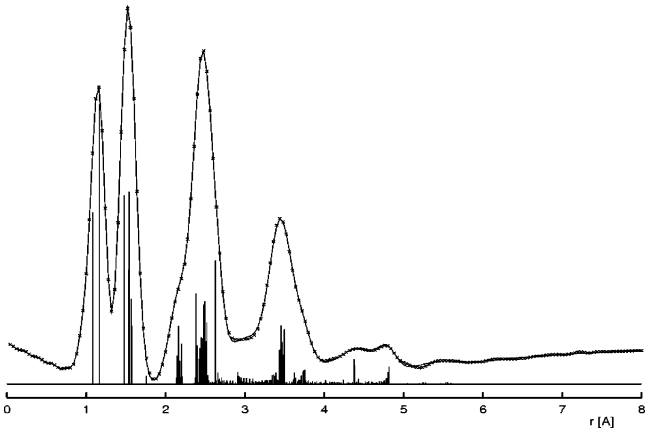

Figure 6. Experimental (×) and theoretical (−) radial distribution function from pseudorotational model for DCCP.

angle φ. The weight function $w(\varphi)$ at temperature T with normalizing factor N is given by

$$w(\varphi) = N \exp(-V(\varphi)/RT)$$

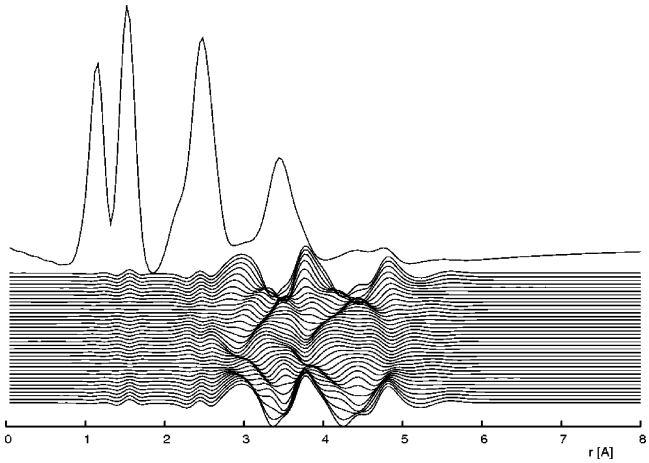

Figure 7. Theoretical total radial distribution function and differences between the contributions from the distinct conformations ($\varphi = 90°$ through $\varphi = +90°$) and the total radial distribution function for DCCP.

To calculate $s*M(s)_{total}$ from eq 10 we set up the geometry of the molecule for various values of the phase angle φ, and calculated the corresponding partial scattering function $M(s,R(\varphi))$. The integrals in eq 10 were subsequently evaluated by numerical integration using the proper subroutine from the NAG library. For symmetry reasons it is sufficient to use an interval width of π. We used a step width of $\delta\varphi = 5°$ in the interval $-90° \leq \varphi \leq +90°$, giving a total of 37 intermediate conformers.

No attempts have been undertaken to extract the potential constants V_2, V_4, or V_6 from the experimental gas electron diffraction data. Instead, the values given in Table 2 were applied. It turns out that the parameters of the HF calculations give slightly better agreement than those of the MP2 calculations.

As before[2] two different types of fitting schemes have been applied to deduce the molecular structure from the electron diffraction patterns using the pseudorotational model: (a) an r_a structure was fitted under the assumption that the r_a parameters

TABLE 8: Comparison of Fitted Structural Parameters in Previous Investigation[2] and in This Work

	ref 2				this work			
	r_a fit		r_α fit		r_a fit		r_α fit	
	value	σ	value	σ	value	σ	value	σ
Geometrical Parameters (Distances in Å, Angles in deg)								
r_{CC}	1.552	0.003	1.549	0.003	1.550	0.003	1.546	0.003
q	0.419	0.049	0.434	0.051	0.437	0.021	0.448	0.021
C−C≡	1.472	0.006	1.472	0.005	1.470	0.006	1.472	0.005
d(C−C≡)	−0.011	0.055	−0.007	fix	0.006	fix	0.006	fix
C≡N	1.164	0.002	1.152	0.002	1.164	0.002	1.149	0.002
C−H	1.085	0.004	1.068	0.004	1.081	0.005	1.065	0.003
α_{512}	104.6	3.2	103.6	3.1	104.3	1.4	103.4	1.2
NC−C−CN	108.9	3.1	109.1	3.7	108.8	2.1	109.6	2.2
H−C−H	113.1	2.7	112.6	2.3	110.0	2.6	109.6	2.0
C−C≡N	173.1	3.2	175.2	3.4	173.1	2.3	174.7	2.3
ρ^a	−6.7	7.0	−4.1	5.6	−4.7	fix	−4.7	fix
Fitted Vibrational Amplitudes (Å)								
l(C−C_{ring})	0.054	0.004	0.055	0.003	0.056	0.003	0.057	0.003
l(C−C≡)	0.041	0.012	0.041	0.006	0.049	0.007	0.048	0.005
l(C−H)	0.079	0.007	0.076	0.006	0.082	0.006	0.079	0.005
l(C≡N)	0.030	0.002	0.029	0.002	0.033	0.002	0.031	0.001
l(C_2···C_4)	0.064	0.032	0.071	0.044	0.077	0.014	0.073	0.012
l(C_2···C_8)	0.068	0.027	0.070	0.026	0.077	0.014	0.073	0.012
l(C3···C_8)	0.073	0.014	0.075	0.013	0.073	fix	0.073	fix
l(C_1···N_7)	0.056	fix	0.056	fix	0.058	0.007	0.054	0.006
l(C_2···N_9)	0.101	0.029	0.104	0.015	0.113	0.013	0.110	0.011
l(C_3···N_9)	0.113	0.022	0.111	0.020	0.095	fix	0.095	fix
l(C_1···H_{10})	0.112	0.006	0.111	0.005	0.109	0.006	0.108	0.004

[a] Rocking angle of $C(CN)_2$ group. fix: parameter not refined.

TABLE 9: Comparison of Bond Distances, Bond Angles and Dihedral Angles (r_a or r_α, Respectively) of 1,1-Dicyanocyclopentane (DCCP) As Obtained from Electron Diffraction and ab Initio Calculations (MP2/6-311+G(2df,2pd))[g]

	r_a fit		r_α fit		ab initio	
	C_s	C_2	C_s	C_2	C_s	C_2
Bond Distances (Å)						
C_1−C_2	1.553(5)	1.575(5)	1.549(5)	1.571(5)	1.544	1.568
C_2−C_3	1.543(4)	1.535(4)	1.539(4)	1.531(4)	1.534	1.526
C_3−C_4	1.556(5)	1.532(5)	1.552 (5)	1.529(5)	1.550	1.525
q^a	0.437(21)	0.443(21)	0.448(21)	0.454(21)	0.443	0.446
C_1−C_6	1.473(6)	1.470(6)	1.475(6)	1.472(5)	1.464	1.461
C_1−C_8	1.468(6)	1.470(6)	1.470(6)	1.472(5)	1.458	1.461
C≡N	1.164(2)	1.164(2)	1.149(1)	1.149(1)	1.171	1.171
⟨C−H⟩[b]	1.081(4)	1.081(4)	1.065(3)	1.065(3)	1.088	1.089
Bond Angles (deg)						
C_1−C_2−C_3	102.7(13)	104.0(12)	102.8(13)	104.4(11)	103.3	104.4
C_2−C_3−C_4	106.3(5)	102.9(9)	106.0(5)	102.3(8)	105.9	102.6
C_5−C_1−C_2	102.5(16)	105.6(16)	101.7(14)	104.8(14)	101.4	104.9
NC−C−CN	109.2(21)	108.6(21)	110.0(22)	109.4(22)	110.3	109.3
⟨H−C−H⟩[b]	110.0(25)	110.0(25)	109.6(20)	109.6(20)	107.9	108.2
β_6 [c]	123.3(14)	125.7(11)	122.9(15)	125.3(11)	121.8	125.3
β_8 [d]	127.5(14)	125.7(11)	127.1(15)	125.3(11)	127.9	125.3
α[e]	43.0(22)		44.0(22)		43.5	
η^f	6.9(23)	6.9(23)	5.3(23)	5.3(23)	2.7	2.5
Dihedral Angles (deg)						
C_1−C_2−C_3−C_4	25.9(13)	36.7(18)	26.7(12)	37.8(17)	26.6	−37.2
C_4−C_5−C_1−C_2	42.1(20)	−13.9 (7)	43.2(20)	−14.4 (5)	42.8	14.2
C_2−C_3−C_4−C_5	0.0	−46.2(21)	0.0	−47.2(21)	0.0	46.6

[a] Puckering amplitude for the ring. [b] Average value. [c] Angle between the bond C_6−C_1 and the plane $C_5C_1C_2$. [d] Angle between the bond C_8−C_1 and the plane $C_5C_1C_2$. [e] Angle between the $C_5C_1C_2$ plane and $C_2C_3C_4C_5$ plane (flap angle). [f] Bending angle (outward) of the C−C≡N chain. [g] Errors in parentheses (in units of last quoted digit) include the error estimates from constant parameters.

are geometrically consistent, and (b) an r_α structure was obtained which is geometrically consistent by definition. The results of both types of fitting are collected in Table 7. Note that this table shows only the values of the parameters included into the fitting process. In Table 7, the different σ values have the following meaning: σ_1 is the single standard error of the fitting procedure, σ_2 is the error propagated from the estimated uncertainties of the fixed parameters, and σ_{total} is the combined final error estimate. The method to calculate the propagated error σ_2 and the total error σ_{total} has been described elsewhere.[16−18] Figure 5 shows the experimental and theoretical reduced molecular intensity $s*M(s)$, and Figure 6 the experimental and theoretical radial distribution function. Finally, Figure 7 shows the differences between the total radial distribution function and

the unweighted partial contributions of the radial distribution functions at different values of the phase angle φ: in this way the effects of the large amplitude treatment can well be visualized.

5. Discussion

Viewing Figure 6, it is apparent that the combination of fitting the zeroth order geometrical parameters with the results of the theoretical calculations in a large amplitude treatment of the pseudorotation provides a consistent description of the experimental electron diffraction data.

Indeed, we find that the overall fit of the experimental data was not significantly improved in comparison to the results presented in the previous paper.[2] However, we could show that the shape of the potential function underlying the analysis of the diffraction data in our previous investigation was basically wrong. With the improved potential function a better fit was obtained through the refinement of a smaller number of parameters. Certainly, the reason for the good quality of the fit in the previous investigation originates from two sources: (i) the dependency of the total reduced intensity function $s*M(s)$ on the potential constants V_2, V_4, and V_6 is very poor, and (ii) the description of the molecular geometry in terms of the geometrical parameters and the functions involved is very similar.

To verify the second point we note the following points: (i) The simple formula for the density function given in ref 2 correctly reproduces the ring C−C bond lengths for $\varphi = 0°$ and $\varphi = 90°$, but it very poorly reproduces these distances at intermediate values of φ. Because of the availability of the full geometry at any value of φ, as was described previously in this paper, the density function could be augmented so that the ring C−C bond lengths are reproduced for the full cycle of the pseudorotation. (ii) To describe the geometry of the $C(CN)_2$ moiety we introduced only higher order terms in this work compared to the previous investigation. (iii) This same argument also holds for the rocking, wagging, and twisting of the CH_2 groups. Thus, if we compare (Table 8) the fitted parameters obtained in the present work and in the former study, we find that these parameters agree well within the error limits. Consequently, there is no need to revise any of the conclusions drawn in the discussion and summary in ref 2.

Finally, since the fitted geometrical parameters in Table 7 in most cases represent the zeroth order Fourier components only, we show in Table 9, for the purpose of comparison, all bond lengths and angles for the C_s symmetry ($\varphi = 0°$) and for the C_2 symmetry ($\varphi = 90°$) together with those obtained from the ab initio calculations at the MP2/6-311+G(2df,2pd) level (taken from ref 2).

One aim of our investigations on geminally substituted cyclopentanes was to explore the influence of the substituents on the geometry of the cyclopentane ring. Therefore, it is interesting to compare the results of the present work with those of the similar work on DClCP. For this purpose we show in Table 3 the coefficients of the density function eq 4 for both molecules DCCP and DClCP. Apparently the parameters r_{CC}, d_1, and d_2 are quite different while all other coefficients are almost identical. In consequence, the variation of the distances in both molecules is almost parallel.

6. Concluding Remarks

Although the reinvestigation of the structure of DCCP has not led to a significantly different result from that we published earlier, however, the expansion of the potential function governing the stability of the conformers (C_s and C_2) describes more precisely the dependency of the structural parameters on the pseudorotational parameter φ. Moreover, the extension of the model, we developed recently[1,2] that correlates the changes of the ring C−C bond lengths upon the fluctuation of the phase angle φ with the variation of the density distribution of the delocalized net charges has led to a more accurate description of this kind of correlation. The augmentation of the underlying equation by new specific terms resulted in the reduction of the observed discrepancy between bond lengths obtained from the quantum mechanical calculations and those emerging from this equation in its original form.

Acknowledgment. M.D. gratefully acknowledges the financial support from the Fonds der Chemischen Industrie.

References and Notes

(1) Dakkouri, M.; Typke, V.; Schauwecker, T. *J. Chem. Phys. A* **2004**, *108*, 4658.
(2) Dakkouri, M.; V. Typke, *J. Mol. Struct.* **2002**, *612*, 181.
(3) Pitzer, K. S. *Science* **1945**, *101*, 672.
(4) Kilpatrick, J. E.; Pitzer, K. S.; Spitzer, R. S. *J. Am. Chem. Soc.* **1947**, *69*, 2483.
(5) Harris, D. O.; Engerholm, G. G.; Tolman, C. A.; Luntz, A. C.; Keller, R. A.; Kim, H.; Gwinn, W. D. *J. Chem. Phys.* **1969**, *50*, 2348.
(6) Laane, J. In *Vibrational Spectra and Structure*; Durig, J. R., Ed.; Marcel Dekker: New York, 1972; Vol. 1, p 25.
(7) Fuchs, B. In *Topics in Stereochemistry*; Eliel, E. L., Allinger, N. L., Eds.; John Wiley & Sons: New York, 1978; Vol. 10, p 1.
(8) Bastiansen, O.; Kveseth, K.; Møllendal, H. In *Topics in Current Chemistry*; Boschke, F. L., Ed.; Springer-Verlag: Berlin, Heidelberg, Germany, and New York, 1979; Vol. 81, p 99.
(9) Strauss, H. L. *Annu. Rev. Phys. Chem.* **1983**, *34*, 301.
(10) Typke, V.; Dakkouri, M.; Oberhammer, H. *J. Mol. Struct.* **1978**, *44*, 85.
(11) Oberhammer, H.; Gombler, W.; Willner, H. *J. Mol. Struct.* **1981**, *70*, 273.
(12) Haase, J. *Z. Naturforsch., Teil A* **1970**, *25*, 936.
(13) *MOLPRO* is a package of ab initio programs: Werner, H.-J.; Knowles, P. J.; Amos, R. D., Bernhardsson, A.; Berning, A.; Celani, P.; Cooper, D. L.; Deegan, M. J. O.; Dobbyn, A. J.; Eckert, F.; Hampel, C.; Hetzer, G.; Knowles, P. J.; Korona, T.; Lindh, R.; Lloyd, A. W.; McNicholas, S. J.; Manby, F. R.; Meyer, W.; Mura, M. E.; Nicklass, A.; Palmieri, P.; Pitzer, R.; Rauhut, G.; Schütz, M.; Schumann, U.; Stoll, H.; Stone, A. J.; Tarroni, R.; Thorsteinsson, T.; Werner, H.-J.
(14) Cremer, D.; Pople, J. A. *J. Am. Chem. Soc.* **1975**, *97*, 1358.
(15) Skancke, P. N.; Fogarasi, G.; Boggs, J. E. *J. Mol. Struct.* **1980**, *62*, 259.
(16) Dakkouri, M.; Typke, V. *J. Mol. Struct.* **1994**, *320*, 13.
(17) Typke, V.; Dakkouri, M.; Schiele, M. *Z. Naturforsch.* **1980**, *35a*, 1402.
(18) Dakkouri, M.; Typke, V. *J. Mol. Struct.* **2000**, *550−551*, 349.